

## Effect of Linear Chirp on Strong Field Photodissociation of $\text{H}_2^+$

Vaibhav S. PRABHUDESAI,\* Adi NATAN, Barry D. BRUNER and Yaron SILBERBERG  
*Department of Physics of Complex Systems, Weizmann Institute of Science, 76100, Israel*

Uri LEV, Oded HEBER, Daniel STRASSER,† Dirk SCHWALM‡ and Daniel ZAJFMAN  
*Department of Particle Physics and Astrophysics, Weizmann Institute of Science, 76100, Israel*

Itzik BEN-ITZHAK

*J. R. Macdonald Laboratory, Department of Physics, Kansas State University, Kansas, 66506, USA*

(Received 2 November 2010, in final form 24 May 2011)

We report the experimental findings of a systematic study of the effect of linear chirp on strong field photodissociation of  $\text{H}_2^+$ . For vibrational levels around or above the one photon crossing, the effect manifests itself in terms of a shift in the kinetic energy release (KER) peaks. The peaks shift up for negative chirp whereas they shift down for positive chirp. The measurements are carried out by varying two of the three laser pulse characteristics, energy, pulse peak intensity and linear chirp, while keeping the third constant. The shifts in the KER peaks are found to be intensity dependent for a given value of chirp. However, in the last two cases (*i.e.*, fixed pulsed energy and fixed pulse peak intensity), they are found to be independent of the chirp magnitude. The results are understood on the basis of saturation of photodissociation probabilities for these levels.

PACS numbers: 33.80.Gj, 34.50.Gb, 34.50.Rk, 42.50.Hz

Keywords: Photodissociation, Strong field, Linear chirp, Kinetic energy release

DOI: 10.3938/jkps.59.2890

### I. INTRODUCTION

Strong field photodissociation of  $\text{H}_2^+$  using ultrashort laser pulses has been extensively studied in recent years [1–11]. All these studies are aimed at improving the understanding of strong field-matter interactions, with a vision of chemical control as the ultimate goal. In this respect, laser peak intensity, pulse duration, central frequency, bandwidth, two-color phase and carrier envelope phase are among the control parameters generally used [4,6,9,11].

Recently, we experimentally demonstrated the possibility of tracing the photodissociation time within the laser pulse using linearly chirped pulses [12]. The photodissociation timing manifests itself in terms of the shift of the kinetic energy release (KER) peaks that are dependent on the intensity and the chirp sign. The effect was understood to stem from the fact that for vibrational levels situated at or above the one-photon crossing of the

dressed ground and the electronic excited states, the photodissociation probability saturates long before the peak of the pulse. This understanding was verified by measuring the effect of the chirp sign and by comparing the experimental results with the numerical solutions of the time dependent Schrödinger equation (TDSE) [12].

Basic characteristics of an ultrafast laser pulse that spans a few tens of femto-seconds include pulse duration, peak intensity and pulse energy. These three parameters are interdependent, and for various values of linear chirp that can be added to the pulse, only one of them can be kept constant. Here, we report a systematic experimental study of the effect of linear chirp on the shift of the KER peaks, keeping each of these parameters constant separately. Specifically, the study includes measurement of KER spectra by (i) varying the pulse energy and, hence, the peak intensity for a given amount of linear chirp, (ii) varying the magnitude of linear chirp and, hence, the peak intensity for a given value of pulse energy, and (iii) varying the pulse energy and linear chirp such that the peak intensity remains constant.

\*E-mail: vaibhav.p.d@gmail.com; Fax: +91-22-2280-4610; Department of Nuclear and Atomic Physics, Tata Institute of Fundamental Research, 400005, India

†Institute of Chemistry, The Hebrew University of Jerusalem, Jerusalem, 91904, Israel

‡Max-Planck-Intitut für Kernphysik, Heidelberg, 69117, Germany

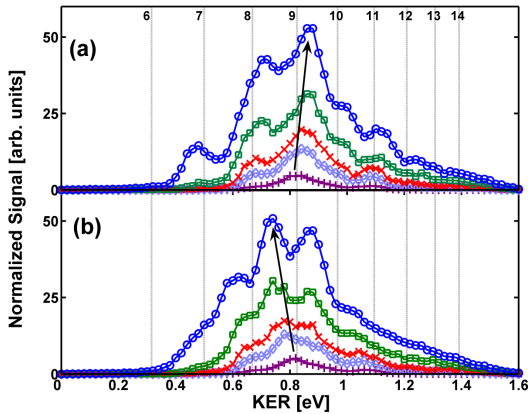


Fig. 1. (Color online) Kinetic energy release spectra of  $\text{H}_2^+$  for (a) negatively and (b) positively chirped pulses taken at different peak intensities of (O)  $2 \times 10^{13}$  W/cm<sup>2</sup>, (□)  $7 \times 10^{12}$  W/cm<sup>2</sup>, (×)  $2 \times 10^{12}$  W/cm<sup>2</sup>, (◇)  $1 \times 10^{12}$  W/cm<sup>2</sup>, and (+)  $1 \times 10^{11}$  W/cm<sup>2</sup> (modified from Fig. 4 of Ref. 12). The spectra are generated by summing the signal over all angles. The solid arrows indicate the direction of the shift in the KER peak position of the  $v = 9$  vibrational level.

## II. EXPERIMENT AND DISCUSSION

The details of the experimental set-up are described elsewhere [12]. In short, the laser beam is crossed with a well-collimated pulsed 4 keV  $\text{H}_2^+$  ion beam in a longitudinal electrostatic spectrometer similar to one used in Ref. 2. The ion beam with a Franck-Condon distribution of vibrational levels is produced in the Neilson ion source [13]. The main ion beam is stopped in front of a time and position sensitive detector (PSD) using a 3mm-diameter Faraday cup. The fragments from photodissociation are detected in coincidence using a 2D PSD comprised of a set of microchannel plates in the Chevron assembly along with a phosphor screen anode, a CCD camera and a homebuilt frame grabber [14]. The characteristics of the intense broadband laser pulses (795 nm, 30 fs (FWHM), at 1 kHz) are well controlled using a conventional 4-f pulse shaper assembly consisting of a programmable liquid crystal spatial light modulator (Jenoptik Phase SLM-640) placed in the Fourier plane of a combination of gratings and cylindrical mirrors [15]. The SLM is used as a dynamic filter for the spectral phase of the pulses [16]. The linearly polarized laser beam is focused onto the ion beam’s crossing point with a focal waist of 80  $\mu\text{m}$  using a 30 cm focal length lens. The direction of the polarization is kept in the plane parallel to that of the particle detector. Using the pulse shaper, we applied a quadratic spectral phase function:  $\Phi(\omega) = \phi''(\omega - \omega_0)^2$ , where  $\phi''$  is the group dispersion delay (GDD) parameter, which corresponds to the linear chirp magnitude, and  $\omega_0$  is the central laser frequency.

In the first set of measurements, the amount of linear chirp (GDD = 630 fs<sup>2</sup>) is adjusted to stretch the pulse duration to 120 fs. In this case, the laser pulse

energy is varied across five different values spanning the peak intensity from  $1 \times 10^{11}$  W/cm<sup>2</sup> to  $2 \times 10^{13}$  W/cm<sup>2</sup>. The measured kinetic energy spectra are shown in Fig. 1. The spectra are comprised of dissociation events corresponding to all the possible orientations of the molecular axis with respect to the laser polarization except for a small angular range around 90° that is blocked by the Faraday cup, which eliminates detection of dissociation events with a very small velocity component perpendicular to the laser polarization or ion beam direction. As can be seen from Fig. 1, the kinetic energy peaks from vibrational levels  $v \geq 8$  show a systematic increase in KER shift with increasing pulse energy. For the lowest intensity pulses ( $I_0 = 1 \times 10^{11}$  W/cm<sup>2</sup>), the KER peak positions coincide with the predicted field-free “vibrational comb”. As the pulse energy increases, the peaks shift monotonically further from the field-free value and in opposite directions for the two chirp signs. In the case of positive chirp, they shift to lower KER values while they shift to higher ones for negative chirp. Measurements with 120 fs narrow bandwidth transform limited laser pulses with similar intensity do not show these shifts, ruling out the role of the Stark effect in these results [12].

The above effect is understood in terms of saturation of the dissociation probability for the above vibrational levels in the presence of a strong laser field. The dissociation probability saturates in the leading edge of the laser pulse long before the pulse peak arrives. As for the positive chirp, the red frequencies precede the blue ones, the peaks shift to the lower energy side of the expected KER position. This reverses for negative chirp, explaining the change in the direction of the KER peak shifts. For a given vibrational level, this saturation takes place at a specific intensity of the laser field that depends on the dipole coupling between the involved electronic states [17]. Consequently, for pulses with higher peak intensity, the dissociation takes place at an even earlier time within the pulse. This translates into an increase in the shift of the KER peak position for a fixed chirp of the laser pulse with increasing peak intensity.

The expected shift in the KER peak is estimated using a simple model. For vibrational level  $v = 9$ , the saturation is estimated to occur for a field intensity of  $1.7 \times 10^{12}$  W/cm<sup>2</sup> according to the TDSE calculations reported earlier [12]. Assuming a Gaussian temporal profile of the laser pulse of a given peak intensity, we evaluated the time of saturation of the dissociation probability. Knowing the GDD of the pulse, we calculated the instantaneous frequency corresponding to this time, which gave an estimate of the magnitude of the shift in the corresponding KER peak. For example, in the case of 120fs pulses with a peak intensity of  $2 \times 10^{13}$  W/cm<sup>2</sup>, this saturation would take place about 100 fs before the peak of the pulse whereas for a peak intensity of  $7 \times 10^{12}$  W/cm<sup>2</sup>, it would precede the pulse peak by about 80fs. This manifests as a change in the shift in the KER peak. Table 1 lists the intensity dependence of the shifts

Table 1. Measured shifts in the KER peak for vibrational level  $v = 9$  with respect to the expected position for the mean frequency of the laser pulse in the weak field limit for different intensities of the laser pulse and a fixed chirp magnitude of  $GDD = 630 \text{ fs}^2$ . The last column lists the magnitude of the shift estimated using the simple model discussed in the text.

Intensity ( $\text{W}/\text{cm}^2$ )	Measured shift in the KER peak (meV)		Estimate of the magnitude of the KER shift (meV)
	for positive chirp	for negative chirp	
$1 \times 10^{12}$	-30	20	0
$2 \times 10^{12}$	-40	30	15
$7 \times 10^{12}$	-60	40	40
$2 \times 10^{13}$	-70	50	53

observed for the  $v = 9$  level for both positive and negative chirp, along with the magnitude of the shift that we estimated using this simple model.

Another feature observed in these spectra is the increase in the relative signal strength in the KER region corresponding to vibrational levels  $v \leq 8$  with respect to the  $v = 9$  peak. This part of the spectra shows a much narrower angular distribution, which is a signature of a strong field effect [12]. The systematic increase in the signal can be attributed to an increase in the peak intensity. The higher peak intensity manifests itself as a larger gap opening between the dressed electronic ground and the excited state of the molecule, increasing the dissociation probability of lower vibrational levels.

The second set of measurements was carried out by varying the magnitude of the linear chirp for laser pulses with fixed energy. The laser pulse gets elongated with linear chirp as

$$\tau^2 = \tau_0^2 + \left( \frac{8 \ln 2 \phi''}{\tau_0} \right)^2, \quad (1)$$

where  $\tau_0$  is the duration of the transform limited pulse,  $\tau$  is the elongated pulse width and  $\phi''$  is the GDD parameter discussed earlier. As a result of this elongation, the peak intensity of the pulse falls as  $1/\tau$ . Figure 2 shows the KER spectra obtained for such pulses. The spectra are recorded, keeping the pulse energy constant at  $170 \mu\text{J}$  which corresponds to a peak intensity of  $2 \times 10^{13} \text{ W}/\text{cm}^2$  for 120 fs pulses. The chirp magnitude is changed to vary the pulse duration from 60 fs to 240 fs.

For this set of measurements as well, we observed that the shifts in the KER peaks for levels  $v \geq 8$  change direction on changing the chirp sign. However, the shifts are not found to depend on the amount of chirp over the range used in these measurements. The shifts of the KER peaks can be explained in terms of dissociation probability saturation, as in the previous case. The lack of a chirp magnitude dependence can be understood as follows: As explained earlier, the increase in the chirp magnitude increases the pulse width and, hence, decreases the peak intensity of the pulse. The decrease in the peak intensity causes the dissociation probability to saturate at a later time within the pulse. However, the increase in chirp magnitude is also associated with a decrease in the frequency sweep rate. This implies that within the range

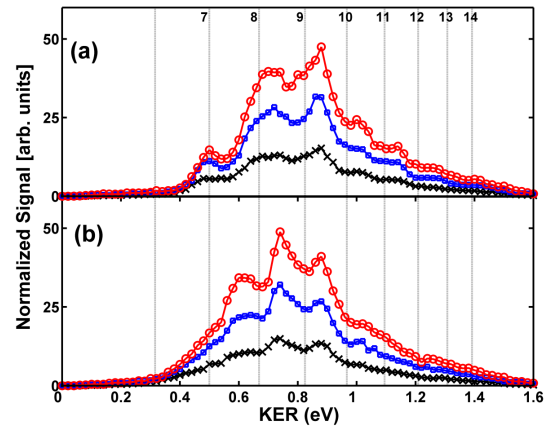


Fig. 2. (Color online) KER spectra of  $\text{H}_2^+$  for (a) negative and (b) positive chirp pulses measured with constant pulse energy ( $170 \mu\text{J}$ , which corresponds to  $2 \times 10^{13} \text{ W}/\text{cm}^2$  peak intensity for 120 fs pulses) with different chirp magnitudes corresponding to (O) 120 fs, ( $\square$ ) 90 fs, and ( $\times$ ) 60 fs pulse widths. The normalized signal is multiplied by a factor of 2 for the 90 fs spectrum and a factor of 3 for the 120 fs data for clarity.

of the chirps used in these measurements, the effect of change in the dissociation time is compensated for by the change in the frequency sweep-rate, explicitly the “photon energy” (at the moment the intensity for saturation of the dissociation probability is reached) remains the same. For the pulse intensities and chirp values used in the experiment, the estimated (by our model) KER shifts and the observed shifts compare well (see Table 2).

Similar behavior is also observed in the third set of measurements in which the chirp and the pulse energy are varied such that the peak intensity remains constant. The KER spectra so obtained for positive and negative chirp are shown in Fig. 3. For the same reason as for the second set of measurements, the KER shifts are unchanged, in agreement with our model calculations (see Table 2).

For the KER region corresponding to levels  $v \leq 8$ , the relative strength of the signal with respect to the  $v = 9$  peak increases with increasing pulse duration. This is understood from the fact that for longer pulses, the avoided gap between the dressed electronic ground and

Table 2. Measured shifts in the KER peak for vibrational level  $v = 9$  with respect to the expected position for the mean frequency of the laser pulse in the weak field limit for different chirp values at constant pulse energy ( $170 \mu\text{J}$ , which corresponds to  $2 \times 10^{13} \text{ W/cm}^2$  at 120 fs pulse width) and at constant peak power ( $2 \times 10^{13} \text{ W/cm}^2$ ). The values are averaged over positive and negative chirp pulses. The last two columns list the magnitude of the shift estimated using the simple model discussed in the text.

Pulse width (fs)	Measured average shift in the KER peak (meV)		Estimate of the magnitude of the shift in the KER peak (meV)	
	for constant pulse energy	for constant peak intensity	for constant pulse energy	for constant peak intensity
	60	70	60	50
90	70	60	55	52
120	70	60	53	53

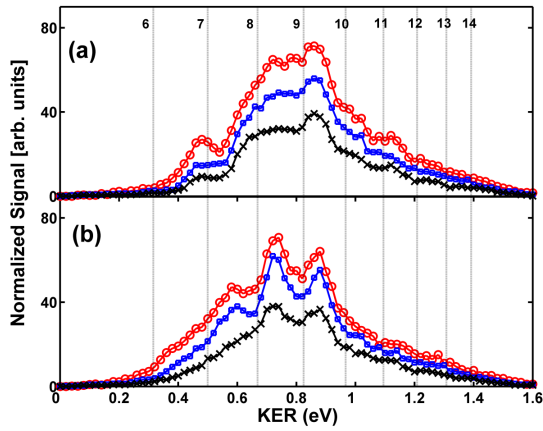


Fig. 3. (Color online) KER spectra of  $\text{H}_2^+$  for (a) negative and (b) positive chirp pulses measured with constant pulse peak intensity ( $2 \times 10^{13} \text{ W/cm}^2$ ) with different chirp values corresponding to pulse durations of (O) 120 fs, ( $\square$ ) 90 fs, and ( $\times$ ) 60 fs.

the excited states opens for a longer time, causing more dissociation.

In all these measurements, a change in the chirp sign causes change in the direction of the shift. This implies that for a purely transform-limited pulse with vanishing chirp, no shift in the KER peaks due to early dissociation is expected, and the major changes in shifts should appear for chirp values that alter the pulse duration by a small amount. This is evident from the simulated shift values for various chirp values shown in Fig. 4, starting from zero and going to the values used in the experiment.

### III. SUMMARY AND CONCLUSION

To summarize, systematic measurements of the effect of linear chirp on strong field photodissociation of  $\text{H}_2^+$  are carried out for laser pulses with (i) constant chirp with different peak intensity and pulse energy, (ii) constant pulse energy and different chirp magnitudes and hence

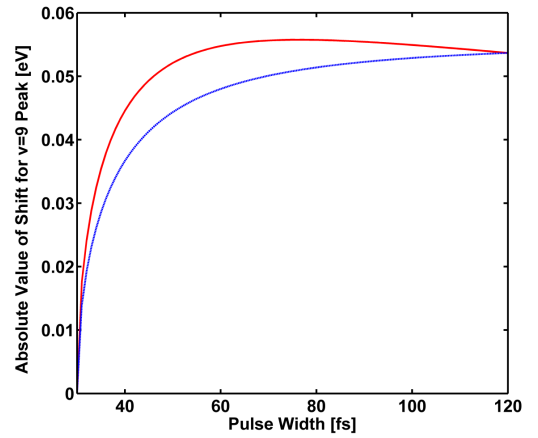


Fig. 4. (Color online) Estimated KER peak shift magnitudes for vibrational level  $v = 9$  using the simple model described in the text for (solid red line) constant pulse energy and (dashed blue line) constant peak intensity as functions of pulse width starting from transform limited. The constant pulse energy was  $170 \mu\text{J}$  (corresponding to a peak intensity of  $2 \times 10^{13} \text{ W/cm}^2$  for a 120 fs pulse), and the constant peak intensity corresponded to  $2 \times 10^{13} \text{ W/cm}^2$  for all the pulses.

different peak intensities and (iii) constant peak intensity with different chirp magnitudes and pulse energies. For vibrational levels  $v \geq 8$ , a shift in the KER peaks is observed, which is attributed to the saturation of the dissociation probability on the rising edge of the laser pulse. The direction of the KER shift changes with the sign of the chirp, confirming the interpretation of the effect. The magnitude of the observed KER shift changes for the first case whereas it remains constant over the range of linear chirp for the last two cases. Clearly, the KER spectral feature obtained in the strong field photodissociation of  $\text{H}_2^+$  not only depends on the pulse duration and the peak intensity but also shows the significant effect of the chirp sign and magnitude. Hence, these factors should be taken into consideration when interpreting the KER spectra of strong field photodissociation experiments, especially when one uses chirp to modify the pulse duration.

### ACKNOWLEDGMENTS

This work was supported by a grant from the G.I.F. (the German-Israeli Foundation for Scientific Research and Development), a grant from the United States-Israel Binational Science Foundation (BSF), Jerusalem, Israel, and a research grant from the Estate of David Turner and the Chemical Sciences, Geosciences, and Biosciences Division, Office of Basic Energy Sciences, Office of Science, U.S. Department of Energy. Dirk Schwalm acknowledges the support by the Weizmann Institute of Science through the Joseph Meyerhoff program.

### REFERENCES

- [1] L. J. Frasinski, J. Plumridge, J. H. Posthumus, K. Codling, P. F. Taday, E. J. Divall and A. J. Langley, *Phys. Rev. Lett.* **86**, 2541 (2001).
- [2] I. Ben-Itzhak, P. Q. Wang, J. F. Xia, A. M. Sayler, M. A. Smith, K. D. Carnes and B. D. Esry, *Phys. Rev. Lett.* **95**, 073002 (2005).
- [3] D. Pavičić, T. W. Hänsch and H. Figger, *Phys. Rev. A* **72**, 053413 (2005).
- [4] M. F. Kling *et al.*, *Science* **312**, 246 (2006).
- [5] D. S. Murphy *et al.*, *J. Phys. B: At. Mol. Opt. Phys.* **40**, S359 (2007).
- [6] J. McKenna, F. Anis, B. Gaire, Nora G. Johnson, M. Zohrabi, K. D. Carnes, B. D. Esry and I. Ben-Itzhak, *Phys. Rev. Lett.* **103**, 103006 (2009).
- [7] F. Kelkensberg *et al.*, *Phys. Rev. Lett.* **103**, 123005 (2009).
- [8] M. Kremer *et al.*, *Phys. Rev. Lett.* **103**, 213003 (2009).
- [9] D. Ray *et al.*, *Phys. Rev. Lett.* **103**, 223201 (2009).
- [10] K. P. Singh *et al.*, *Phys. Rev. Lett.* **104**, 023001 (2010).
- [11] C. R. Calvert, W. A. Bryan, W. R. Newell and I. D. Williams, *Phys. Rep.* **491**, 1 (2010), and references therein.
- [12] V. S. Prabhudesai *et al.*, *Phys. Rev. A* **81**, 023401 (2010).
- [13] K. O. Nielsen, *Nucl. Instrum.* **1**, 289 (1957).
- [14] D. Strasser, K. G. Bhushan, H. B. Pedersen, R. Wester, O. Heber, A. Lafosse, M. L. Rappaport, N. Alstein and D. Zajfman, *Phys. Rev. A* **61**, 060705(R) (2000).
- [15] A. M. Weiner, *Rev. Sci. Instrum.* **71**, 1929 (2000).
- [16] N. Dudovich, B. Dayan, S. M. G. Faeder and Y. Silberberg, *Phys. Rev. Lett.* **86**, 47 (2001).
- [17] F. Anis, T. Cackowski and B. D. Esry, *J. Phys. B* **42**, 091001 (2009).